

## MICROBIAL METABOLISM

# Methane metabolism in the archaeal phylum Bathyarchaeota revealed by genome-centric metagenomics

Paul N. Evans,<sup>1\*</sup> Donovan H. Parks,<sup>1\*</sup> Grayson L. Chadwick,<sup>2</sup> Steven J. Robbins,<sup>1</sup> Victoria J. Orphan,<sup>2</sup> Suzanne D. Golding,<sup>3</sup> Gene W. Tyson<sup>1,4,†</sup>

Methanogenic and methanotrophic archaea play important roles in the global flux of methane. Culture-independent approaches are providing deeper insight into the diversity and evolution of methane-metabolizing microorganisms, but, until now, no compelling evidence has existed for methane metabolism in archaea outside the phylum Euryarchaeota. We performed metagenomic sequencing of a deep aquifer, recovering two near-complete genomes belonging to the archaeal phylum Bathyarchaeota (formerly known as the Miscellaneous Crenarchaeotal Group). These genomes contain divergent homologs of the genes necessary for methane metabolism, including those that encode the methyl-coenzyme M reductase (MCR) complex. Additional non-euryarchaeotal MCR-encoding genes identified in a range of environments suggest that unrecognized archaeal lineages may also contribute to global methane cycling. These findings indicate that methane metabolism arose before the last common ancestor of the Euryarchaeota and Bathyarchaeota.

**A**naerobic archaea are major contributors to global methane cycling. Methanogenic archaea are estimated to produce one billion tons of methane per year, with an equal amount estimated to be oxidized by archaeal methanotrophs (1). All previously described archaeal methane-metabolizing microorganisms belong to the phylum Euryarchaeota (2) and share a core set of bidirectional enzymes responsible for their respective metabolisms (3). This restricted phylogenetic distribution has led to the hypothesis that archaeal methane metabolism originated within the Euryarchaeota (4), although an origin outside this phylum has also been proposed (5). Recent advances in metagenomic techniques are allowing population genomes to be recovered en masse across many previously uncultivated archaeal lineages and from increasingly complex environments (6, 7). This has greatly expanded our understanding of the metabolic capabilities of these lineages; however, no methanogenic or methanotrophic archaea have been discovered thus far outside of the Euryarchaeota phylum.

The recently proposed Bathyarchaeota phylum (formerly the Miscellaneous Crenarchaeotal Group, MCG) represents an evolutionarily diverse group of microorganisms (8–11) found in a wide range of environments, including deep-

ocean and freshwater sediments (9, 12, 13). The high abundance of bathyarchaeotal 16S ribosomal RNA (rRNA) genes and lipid biomarkers within sulfate-methane transition zones has led to speculation that members of this lineage may be involved in dissimilatory anaerobic oxidation of methane, coupled to organic carbon assimilation (14). However, no Bathyarchaeota have been successfully cultured, and the only genomic representative is a ~21% complete single-cell genome, AB-536-E09 (E09), which was obtained from marine sediments (13). Although the E09 genome appears to belong to a peptide fermenter, its full metabolic potential is not understood because of its genome being incomplete. Given the wide environmental and phylogenetic diversity of Bathyarchaeota, additional genomes are required

to understand the metabolic capabilities of this understudied phylum.

In this study, we collected microbial biomass from filtered formation waters in 11 coal-bed methane wells within the Surat Basin (Queensland, Australia; fig. S1). Recovered DNA was sequenced, assembled, and binned into population genomes (supplementary materials). From the CX-10 sample, 19 population genomes were recovered (table S1), including two Bathyarchaeota genomes estimated to be ~92% (BA1) and ~94% (BA2) complete, as determined by the presence of single-copy marker genes (Table 1). A genome tree, inferred from 144 phylogenetically informative genes, places the BA1 and BA2 genomes and the E09 single-cell genome in a well-supported phylum that is sister to the Thaumarchaeota and Aigarchaeota phyla (Fig. 1A). The 16S rRNA gene tree is congruent with the genome tree and places these genomes with environmental clones belonging to Bathyarchaeota (Fig. 1B). The BA1 and BA2 genomes only share 656 genes (31.5%), with an average amino acid identity of 67.0%, and they have a 16S rRNA sequence identity of 90.5% (table S2), indicating that they represent separate genera or families (15, 16). E09 represents a distinct bathyarchaeotal family from BA1 and BA2, based on 16S rRNA sequence identity (81.5% to BA1, 83.5% to BA2), and shares 56 of its 603 genes (9.3%) with these genomes (fig. S2 and table S3).

Metabolic reconstruction of the BA1 genome revealed the presence of many genes in the Wood-Ljungdahl pathway and key genes associated with archaeal methane metabolism (Fig. 2 and table S4)—most importantly, those that encode the methyl-coenzyme M reductase complex (MCR) (*mcrABG* and putatively *mcrCD*; supplementary text). The BA1 genome contains genes for methanogenesis from methyl sulfides (*mtsA*), methanol (*mtbA*), and methylated amines (*mtaA*, *mttBC*, *mtbBC*), as well as three *mtrH* subunits, each collocated with a corrinoid protein (Fig. 2). The presence of these genes suggests the potential for diverse methyl compound utilization,

**Table 1. Summary statistics of Bathyarchaeota genomes.**

	BA1 (this study)	BA2 (this study)	E09 [from (13)]
Completeness*	91.6%	93.8%	21.5%
Contamination*	2.8%	3.7%	0.0%
Total length (base pairs)	1,931,714	1,455,689	529,171
GC content	47.1%	44.2%	43.3%
Number of scaffolds	89	57	87
Number of contigs	96	58	87
N50 of contigs	32,677	43,519	13,721
Number of coding sequences†	2403	1761	603
Coding density	80.8%	83.6%	81.7%
Average coverage	35.8	49.8	no data
Relative abundance‡	0.92%	1.03%	no data

\*Based on lineage-specific marker sets determined with CheckM (28). †Inferred with Prodigal (29). ‡Estimated from the proportion of reads mapped to the genome.

<sup>1</sup>Australian Centre for Ecogenomics, School of Chemistry and Molecular Biosciences, University of Queensland, St Lucia 4072, Queensland, Australia. <sup>2</sup>Division of Geological and Planetary Sciences, California Institute of Technology, Pasadena, CA 91125, USA. <sup>3</sup>School of Earth Sciences, University of Queensland, St Lucia 4072, Queensland, Australia. <sup>4</sup>Advanced Water Management Centre, University of Queensland, St Lucia 4072, Queensland, Australia. \*These authors contributed equally to this work. †Corresponding author. E-mail: g.tyson@uq.edu.au

similar to that found in obligate H<sub>2</sub>-utilizing methylotrophic methanogens belonging to the order Methanomassiliococcales (17). Additionally, these genes may be sufficient for methyl group transfer directly to tetrahydromethanopterin (H<sub>4</sub>MPT) for carbon assimilation (18). Further, 12 novel methyltransferases with high similarity to each other, but divergent from known methyltransferases, were also identified in the genome, suggesting that this microorganism may use additional methylated compounds. However, the absence of most subunits of the Na<sup>+</sup>-translocating methyl-H<sub>4</sub>MPT:coenzyme M methyltransferase (MTR; encoded by *mtrABCDEFGHI*) suggests that BA1 is unable to perform hydrogenotrophic methanogenesis.

BA1 also contains genes (*hdrABC* and *mvhADG*) that encode a conventional heterodisulfide reductase-F<sub>420</sub> nonreducing hydrogenase electron-bifurcating complex, which is needed for the cycling of coenzyme M (CoM) and coenzyme B (CoB). In addition, three copies of the gene for heterodisulfide reductase subunit D (*hdrD*) were found collocated with the gene for cytoplasmic flavin adenine dinucleotide-containing dehydrogenases (*gldD*), a gene arrangement also found in the lactate utilization operon of *Archaeoglobus fulgidis* (19). This indicates that lactate may also

serve as an electron donor for the reduction of the heterodisulfide in methanogenesis, functionally replacing methanophenazine and HdrE as the source of electrons for HdrD. The absence of HdrE is also seen in some methylotrophic methanogens belonging to the recently described order Methanomassiliococcales, which also lack the genes for the MTR complex (17). In addition to the missing MTR subunits, the BA1 genome also lacks most other energy-conserving complexes, including the F<sub>420</sub>H<sub>2</sub> dehydrogenase (encoded by *fpo*), energy-converting hydrogenases A and B (*eha* and *ehb*), Rhodobacter Nitrogen Fixation complex, and V/A-type adenosine triphosphate (ATP) synthase. The only complex capable of conserving energy via ion pumping is an energy-converting hydrogenase (encoded by *ech*), which may be sufficient for energizing the membrane for solute transport in the absence of energy-generating mechanisms. To ensure that our results did not reflect contamination within the BA1 population genome, we examined contigs encoding genes associated with methane metabolism to ensure that they agreed with the average guanine-cytosine (GC) content, coverage, and tetranucleotide frequencies of the genome (fig. S3).

Similar to BA1, the BA2 genome contains genes that encode the MCR complex (*mcraBGC*) and

a number of additional genes typical of methane metabolism (*hdrABC*, *hdrD*, and *mvhADG*) (Fig. 2 and fig. S4). These include homologs to the genes for the novel methyltransferases found in BA1, suggesting that BA2 may also be capable of methylotrophic methanogenesis. However, in contrast to BA1, the majority of genes involved in the methyl branch of the Wood-Ljungdahl pathway either were not identified or appeared to be repurposed. For example, the gene for formylmethanofuran:H<sub>4</sub>MPT formyltransferase (*ftr*) was present in the BA2 genome, but it was found in an operon for purine biosynthesis and may have been co-opted into the formyl transferase reactions in this pathway. Additionally, the H<sub>4</sub>MPT biosynthesis genes (*mptBN*) have greater sequence similarity to bacterial homologs than to euryarchaeotal or BA1 homologs. Chemiosmotic energy-conserving complexes were also absent in the BA2 genome, including the energy-conserving hydrogenase complex (*ech*) found in BA1.

In addition to the differences between their methane-metabolism pathways, comparative genomic analysis identified other metabolic differences between the BA1 and BA2 genomes. Similar to the peptide-fermenting lifestyle inferred from the E09 single-cell genome (13), BA1 can generate acetyl-coenzyme A (CoA) from oxidative

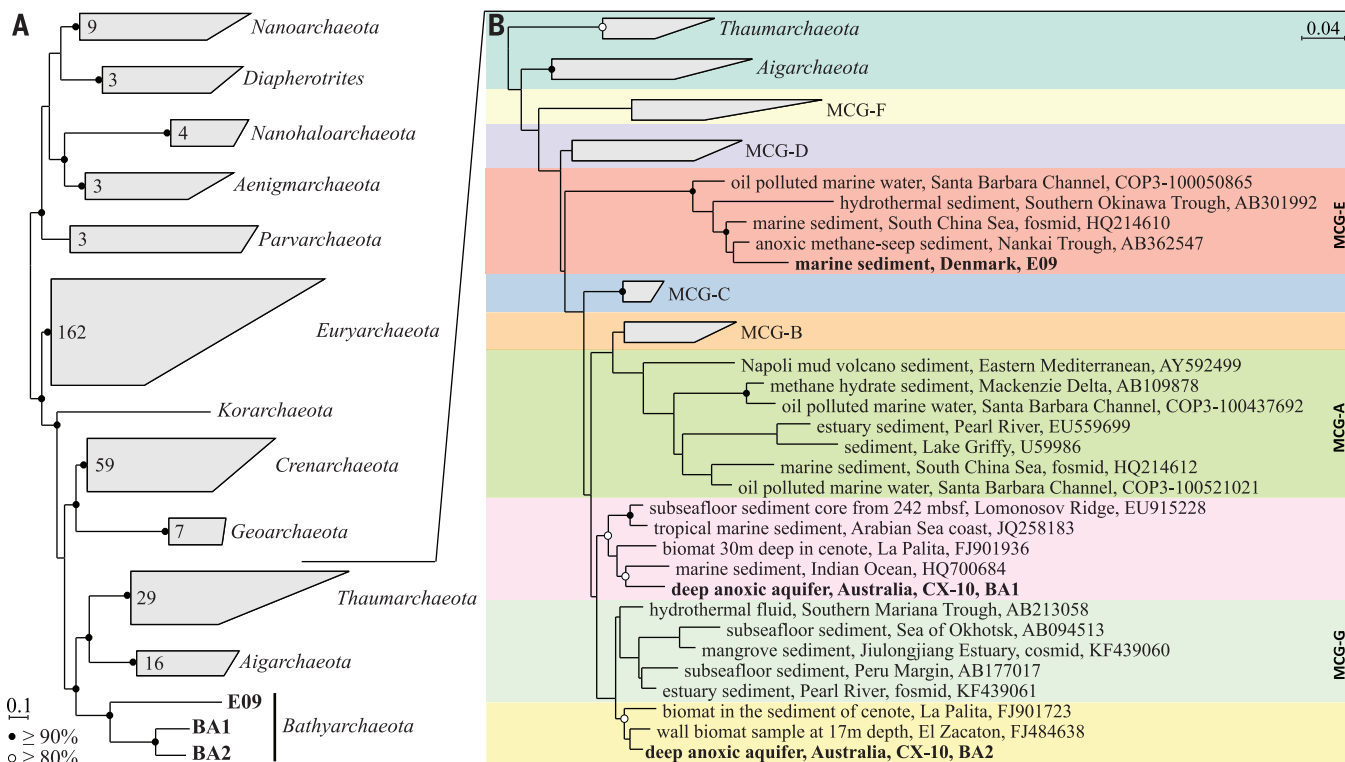


**Fig. 1. Phylogenetic trees showing the placement of the BA1, BA2, and E09 genomes in the archaeal phylum Bathyarchaeota.**

**(A)** Maximum-likelihood tree of 295 archaea, inferred from a concatenated alignment of 144 proteins and rooted with the DPANN (Diapherotrites Parvarchaeota Aenigmarchaeota Nanoarchaeota Nanohaloarchaeota) superphyla (27). Support values are shown with white ( $\geq 80\%$ ) and black ( $\geq 90\%$ ) circles and indicate the minimum support under nonparametric bootstrapping, gene jackknifing, and taxon jackknifing (supplementary materials). **(B)** Maximum-likelihood 16S rRNA gene tree

showing the placement of bathyarchaeotal representatives relative to environmental sequences, including genes recovered from Coal Oil Point. Thaumarchaeota and Aigarchaeota 16S rRNA sequences from reference genomes were used as an outgroup. Bathyarchaeota (formerly MCG) groups are based on the classification in (9). Nonparametric support values are shown with white ( $\geq 80\%$ ) and black ( $\geq 90\%$ ) circles. Environmental context and genomes or National Center for Biotechnology Information accession numbers are given. Scale bars indicate expected number of substitutions per site.

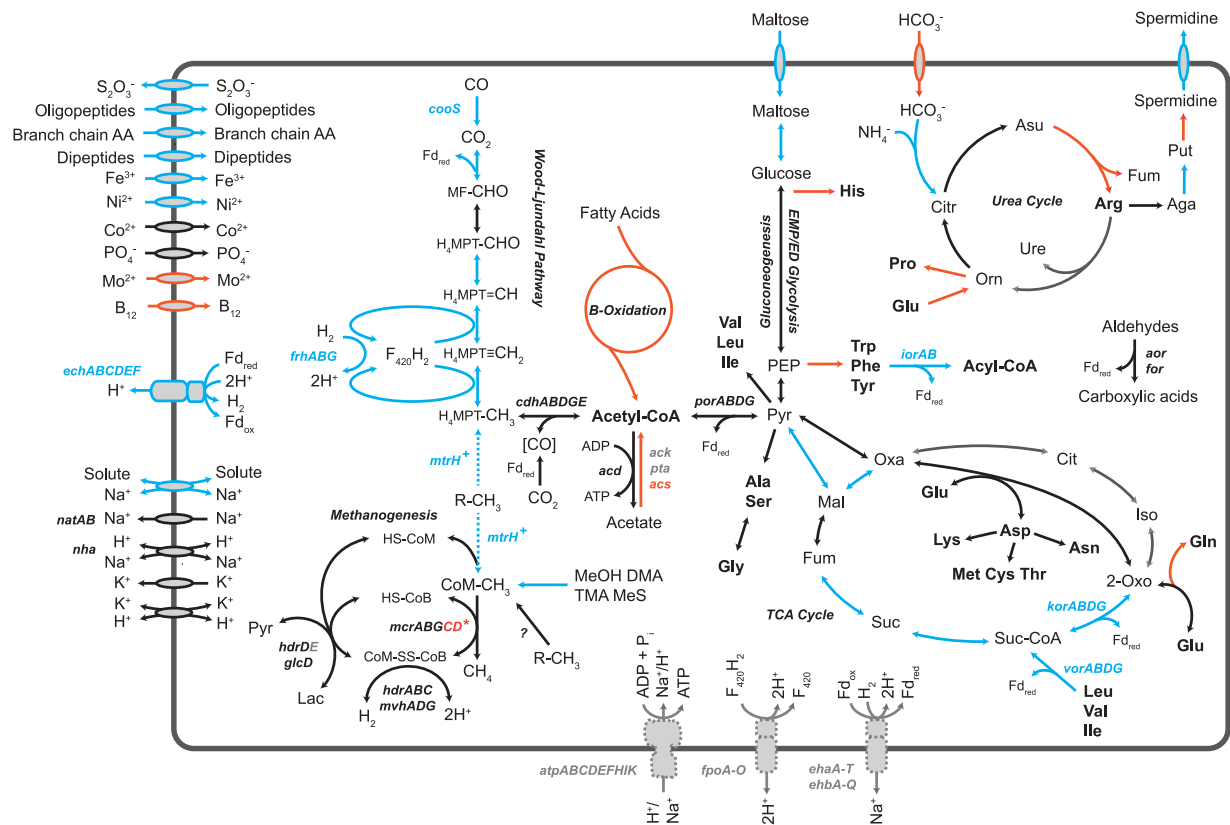


**Fig. 2. Key metabolic pathways in the BA1 and BA2 genomes.** Genes and pathways found in both BA1 and BA2 (black), only found in BA1 (blue), only found in BA2 (orange), or missing from both genomes (gray) are indicated. Genes associated with the pathways highlighted in this figure are presented in tables S9 (BA1) and S10 (BA2). In the BA1 genome, *\*mtrH* genes are adjacent to corrinoid proteins. A bathyarchaeotal contig containing *mcrCD* genes was identified in the metagenome, which probably belongs to the BA1 genome (supplementary text). EMP/ED, Embden-Meyerhof-Parnas/Entner–Doudoroff pathway; TCA, tricarboxylic acid.

deamination of amino acids by glutamate dehydrogenase (encoded by *gdh*), aspartate aminotransferases (*aspC*), and 2-oxoacid:ferredoxin oxidoreductases (*kor*, *ior*, *por*, and *vor*). Aldehydes generated by these oxidoreductases can also be used to generate reduced ferredoxin and oxoacids via multiple aldehyde:ferredoxin oxidoreductases (*aor* or *for*) (20). Consistent with peptide fermentation, the BA1 genome contains multiple peptidases and amino acid and oligopeptide transporters (Fig. 2). Acetyl-CoA generated in the above reactions, or through the reductive acetyl-CoA pathway, can be used for ATP formation through the adenosine diphosphate (ADP)-forming acetyl-CoA synthase (encoded by *ack*). The BA1 genome also contains a putative maltose transporter and an  $\alpha$ -1-4 glycosyl hydrolase (GH family 38), indicating that glucose may be used as a carbon or energy source. Similar characteristics of peptide fermentation and maltose utilization are seen in *Pyrococcus* and other nonmethanogenic archaea (20). In contrast, BA2 appears to be a fatty-acid oxidizer, generating ATP from acetyl-CoA formed through  $\beta$ -oxidation and oxidation of pyruvate via the pyruvate:ferredoxin oxidoreductase (encoded by *por*). Genes for acetate assimilation via phosphotransacetylase (*pta*) or acetate kinase (*ack*) were not identified in either

genome. BA2 is predicted to be able to synthesize all 20 standard amino acids, whereas BA1 appears to be auxotrophic for histidine, proline, tryptophan, tyrosine, and phenylalanine, consistent with its ability to take up amino acids from the environment (Fig. 2).

MCR is the only catabolic enzyme shared by all methane-metabolizing organisms and has not previously been identified in microorganisms outside Euryarchaeota. To further explore the distribution and diversity of this complex, *mcrA* gene sequences from BA1 and BA2 were used to identify homologs across the Surat Basin and 2705 publicly available metagenomes. Non-euryarchaeotal *mcrA* genes were recovered from 8 of the 11 Surat Basin samples, and these genes cluster with those from BA1 and BA2 (Fig. 3 and table S5). An additional five nearly full-length *mcrA* genes were recovered from hydrocarbon-seep samples from Coal Oil Point (Santa Barbara, California), and these sequences constitute sister lineages to the Surat Basin *mcrA* sequences (Fig. 3 and table S5). Non-euryarchaeotal *mcrA* gene fragments (50 to 98% amino acid similarity) were also identified in other high-methane flux environments, including tar sand tailing ponds (Alberta, Canada), petroleum reservoir sediments (North Sea, UK), and several aquatic environments (table S6).

These results show that there is substantial *mcrA* diversity outside of the Euryarchaeota phylum, which may even extend beyond the Bathyarchaeota phylum. This diversity has previously gone unrecognized, because commonly used polymerase chain reaction primers for *mcrA* fail to amplify these divergent genes (fig. S5). Our results also indicate that not all Bathyarchaeota encode *mcrA*. Bathyarchaeotal *mcrA* genes were not identified in many metagenomes, where a substantial proportion of the community were inferred to belong to this phylum (table S7), which explains conflicting observations about Bathyarchaeota and their role in methane metabolism (11, 21). Consistent with the MCR subunit A (McrA) tree (Fig. 3), trees for McrB and McrG show substantial divergence between euryarchaeotal sequences and homologs from the Surat Basin and Coal Oil Point, including the gene sequences identified within the BA1 and BA2 genomes (figs. S6 to S8). The congruent topologies of these gene trees support the hypothesis that the MCR complex has coevolved as a functional unit and that methane metabolism was present in the last common ancestor of Euryarchaeota and Bathyarchaeota.

Despite the divergence of these novel *McrA* genes from their euryarchaeotal homologs (Fig. 3), they appear to be functionally conserved. The

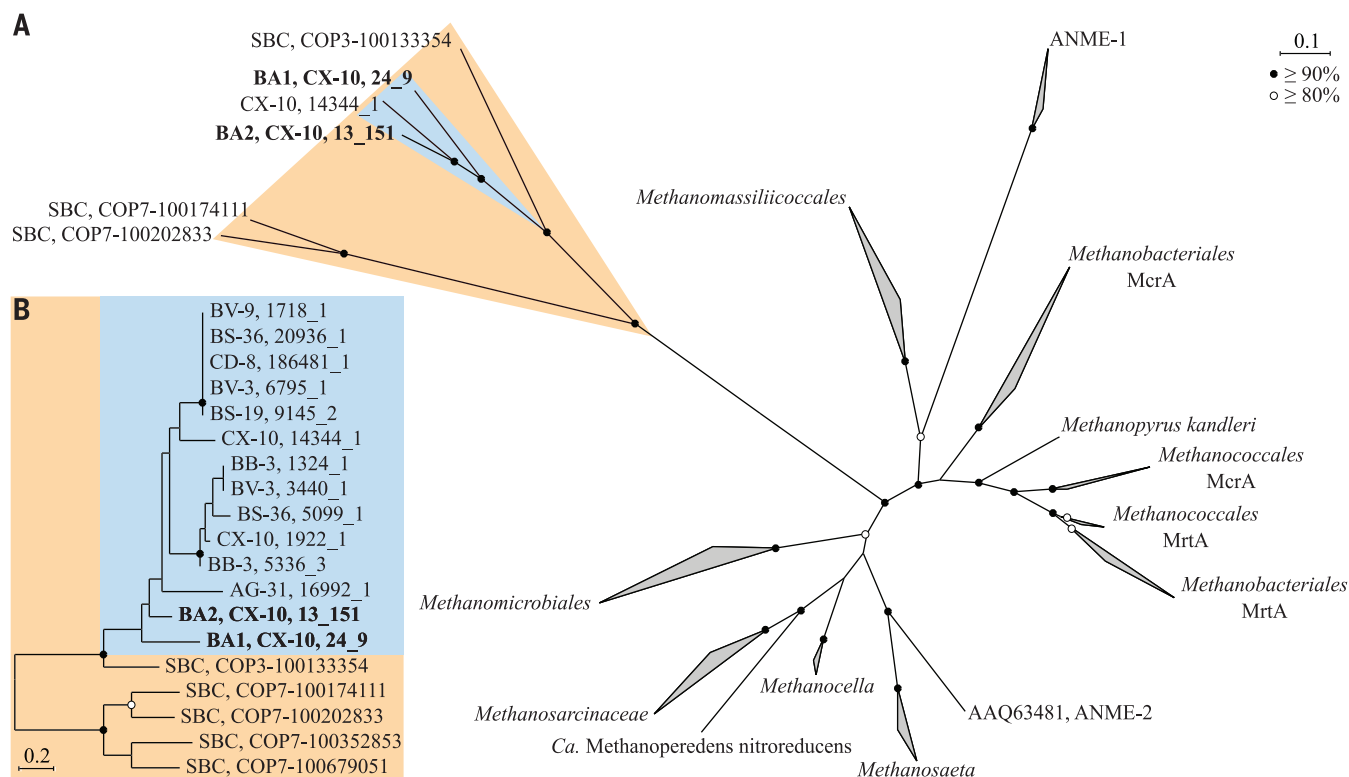


**Fig. 3. Maximum-likelihood trees of McrA.** (A) Placement of nearly full-length McrA protein sequences ( $\geq 400$  amino acids) identified within the Surat Basin and Coal Oil Point metagenomes, in relation to 153 proteins obtained from GenBank. Lineages were collapsed (depicted as wedges) and labeled according to the lowest common ancestor of all taxa in the lineage. (B) Maximum-likelihood tree of nearly full-length and partial McrA sequences identified within the Surat Basin and Coal Oil Point metagenomes. Nonparametric support values are shown with white ( $\geq 80\%$ ) and black ( $\geq 90\%$ ) circles. Information about the Surat Basin wells is given in fig. S1. SBC, Santa Barbara Channel.

ligand-binding sites for CoB, CoM, and cofactor  $F_{430}$  (22) are largely conserved or have complementary amino acid substitutions to extant proteins (fig. S9 and table S8). Additionally, all functionally important residues in McrB and McrG proteins are conserved across the BA1 and BA2 proteins and their euryarchaeotal homologs (table S8). This strongly suggests that the MCR complex in these genomes can perform the same chemistry as its euryarchaeotal counterparts. Structure prediction of the McrA, McrB, and McrG proteins within the BA1 genome revealed high conservation with the crystal structures from *Methanopyrus kandleri* (fig. S10), indicating the potential for protein-ligand binding of CoB, CoM, and  $F_{430}$  (fig. S11). Despite the absence of almost all genes required for the synthesis of CoM and CoB in BA1 and BA2 (tables S9 and S10), these compounds remain the most likely substrates, based on the conserved nature of the MCR active sites. An N-terminal extension and a 19-amino acid insertion specific to the non-euryarchaeotal McrA protein sequences reside close to each other in the tertiary structure, despite being separated by  $\sim 300$  amino acids in the primary sequence, suggesting that these may be involved in novel interactions with other protein complexes (fig. S10). Additionally, BA2 contains a homolog of the ATP-binding protein AtwA (component A2) that was recently shown to be necessary for MCR

activation in vitro (23), providing further evidence that a functional MCR complex is present in Bathyarchaeota (table S10).

The ability of BA1 and BA2 to carry out complex fermentation and  $\beta$ -oxidation, respectively, is unique among archaeal methanogens and methanotrophs (2). The presence of methane-metabolizing genes in a genome capable of complex fermentation leads us to hypothesize that BA1 is a methylotrophic methanogen that uses reduced ferredoxin, generated during fermentation of amino acids and maltose, to reduce methyl groups from diverse organic sources to methane (Fig. 2 and supplementary text). In contrast, we predict that BA2 derives its energy from fatty acid metabolism, and the presence of a gene for acetyl-CoA synthase (*acs*) suggests that carbon can be incorporated into biomass from acetate. However, like BA1, BA2 also appears to have the potential for methylotrophic methanogenesis using a wide range of methylated compounds (Fig. 2). Both BA1 and BA2 appear to lack ATP synthase genes, suggesting that they are restricted to substrate-level phosphorylation to gain energy. Although bacterial and archaeal genomes lacking ATP synthase genes have been recovered from a contaminated aquifer (7, 24), the absence of these genes in microorganisms with a methanogenic lifestyle is unexpected. These genes may be contained in the missing fraction

(<10%) of the BA1 or BA2 genome, although this is unlikely, because they are absent in both genomes and could not be identified in the metagenomic data. Given the outstanding questions about these bathyarchaeotal genomes and the bidirectionality of the enzymes involved in archaeal methane metabolism, it remains possible that these organisms could gain energy from the oxidation of methane (14). Although no genes were identified for coupling methane oxidation to known electron acceptors (25, 26), it is possible that  $CO_2$  could act as an electron acceptor in the reversal of acetoclastic methanogenesis, producing acetate for a syntrophic association (supplementary text). The discovery of bathyarchaeotal and non-euryarchaeotal methane-metabolizing lineages has potentially important consequences for our understanding of the carbon cycle and directly affects our interpretation of the origin and evolutionary history of the MCR complex.

#### REFERENCES AND NOTES

1. W. Reebergh, *Chem. Rev.* **107**, 486–513 (2007).
2. R. K. Thauer, A. K. Kaster, H. Seedorf, W. Buckel, R. Hedderich, *Nat. Rev. Microbiol.* **6**, 579–591 (2008).
3. R. K. Thauer, *Curr. Opin. Microbiol.* **14**, 292–299 (2011).
4. S. Gribaldo, C. Brochier-Armanet, *Philos. Trans. R. Soc. London B Biol. Sci.* **361**, 1007–1022 (2006).
5. S. Kelly, B. Wickstead, K. Gull, *Proc. Biol. Sci.* **278**, 1009–1018 (2011).
6. V. Iverson *et al.*, *Science* **335**, 587–590 (2012).
7. C. J. Castelle *et al.*, *Curr. Biol.* **25**, 690–701 (2015).

8. E. J. Gagen, H. Huber, T. Meador, K. U. Hinrichs, M. Thomm, *Appl. Environ. Microbiol.* **79**, 6400–6406 (2013).
9. J. Meng *et al.*, *ISME J.* **8**, 650–659 (2014).
10. C. S. Lazar *et al.*, *Environ. Microbiol.* **17**, 2228–2238 (2015).
11. K. Kubo *et al.*, *ISME J.* **6**, 1949–1965 (2012).
12. C. Vetriciani, H. W. Jannasch, B. J. MacGregor, D. A. Stahl, A. L. Reysenbach, *Appl. Environ. Microbiol.* **65**, 4375–4384 (1999).
13. K. G. Lloyd *et al.*, *Nature* **496**, 215–218 (2013).
14. J. F. Biddle *et al.*, *Proc. Natl. Acad. Sci. U.S.A.* **103**, 3846–3851 (2006).
15. K. T. Konstantinidis, J. M. Tiedje, *Proc. Natl. Acad. Sci. U.S.A.* **102**, 2567–2572 (2005).
16. P. Yarza *et al.*, *Nat. Rev. Microbiol.* **12**, 635–645 (2014).
17. K. Lang *et al.*, *Appl. Environ. Microbiol.* **81**, 1338–1352 (2015).
18. U. Harms, R. K. Thauer, *Eur. J. Biochem.* **250**, 783–788 (1997).
19. W. P. Hocking, R. Stokke, I. Roalkvam, I. H. Steen, *Front. Microbiol.* **5**, 95 (2014).
20. K. Ma, A. Hutchins, S. J. Sung, M. W. Adams, *Proc. Natl. Acad. Sci. U.S.A.* **94**, 9608–9613 (1997).
21. J. F. Biddle, S. Fitz-Gibbon, S. C. Schuster, J. E. Brenchley, C. H. House, *Proc. Natl. Acad. Sci. U.S.A.* **105**, 10583–10588 (2008).
22. U. Ermiler, W. Grabarse, S. Shima, M. Goubeaud, R. K. Thauer, *Science* **278**, 1457–1462 (1997).
23. D. Prakash, Y. Wu, S. J. Suh, E. C. Duin, *J. Bacteriol.* **196**, 2491–2498 (2014).
24. C. T. Brown *et al.*, *Nature* **523**, 208–211 (2015).
25. M. F. Haroon *et al.*, *Nature* **500**, 567–570 (2013).
26. E. J. Beal, C. H. House, V. J. Orphan, *Science* **325**, 184–187 (2009).
27. C. Rinke *et al.*, *Nature* **499**, 431–437 (2013).
28. D. H. Parks, M. Imelfort, C. T. Skennerton, P. Hugenholtz, G. W. Tyson, *Genome Res.* **25**, 1043–1055 (2015).
29. D. Hyatt *et al.*, *BMC Bioinformatics* **11**, 119 (2010).

## ACKNOWLEDGMENTS

We thank E. Gagen and P. Hugenholtz for valuable comments and suggestions; K. Baublys, SGS-Leeder, and Australian Laboratory Services staff for sample collection; and M. Butler and S. Low for library preparation and sequencing. This study was supported by the Australian Research Council (ARC) Linkage Project (grant LP100200730) and the U.S. Department of Energy's Office of Biological Environmental Research (award no. DE-SC0010574). D.H.P. is supported by the Natural Sciences and Engineering

Research Council of Canada. S.J.R. is supported by an Australian Postgraduate Award Industry scholarship. G.W.T. is supported by an ARC Queen Elizabeth II Fellowship (grant DP1093175). The authors declare no conflicts of interest. Our Whole Genome Shotgun projects have been deposited in the DNA DataBank of Japan, the European Molecular Biology Laboratory repository, and NIH's GenBank under the accession numbers LIHJ00000000 (BA1) and LIHK00000000 (BA2). The versions described in this paper are LIHJ01000000 (BA1) and LIHK01000000 (BA2). Non-euryarchaeotal Surat Basin *mcrA* sequences have been deposited under the accession numbers KT387805 to KT387832, and unprocessed reads have been deposited under the accession number SRX1122679.

## SUPPLEMENTARY MATERIALS

www.sciencemag.org/content/350/6259/434/suppl/DC1  
Materials and Methods  
Supplementary Text  
Figs. S1 to S14  
Tables S1 to S13  
References (30–87)

11 June 2015; accepted 14 September 2015  
10.1126/science.aac7745

## PLANT SCIENCE

# Mechanosensitive channel MSL8 regulates osmotic forces during pollen hydration and germination

Eric S. Hamilton, Gregory S. Jensen, Grigory Makshev, Andrew Katims,\*  
Ashley M. Sherp, Elizabeth S. Haswell†

Pollen grains undergo dramatic changes in cellular water potential as they deliver the male germ line to female gametes, and it has been proposed that mechanosensitive ion channels may sense the resulting mechanical stress. Here, we identify and characterize MscS-like 8 (MSL8), a pollen-specific, membrane tension-gated ion channel required for pollen to survive the hypoosmotic shock of rehydration and for full male fertility. MSL8 negatively regulates pollen germination but is required for cellular integrity during germination and tube growth. MSL8 thus senses and responds to changes in membrane tension associated with pollen hydration and germination. These data further suggest that homologs of bacterial MscS have been repurposed in eukaryotes to function as mechanosensors in multiple developmental and environmental contexts.

**M**echanosensitive (stretch-activated) ion channels provide an evolutionarily conserved mechanism for the perception of mechanical force at the membrane (1). The mechanosensitive channel of small conductance (MscS) from *Escherichia coli* belongs to a large and structurally diverse family of proteins encoded in bacterial, archaeal, plant, and fungal genomes (2, 3). Bacterial MscS homologs prevent cellular lysis upon hypoosmotic shock by releasing osmolytes from the cell in direct response to increased lateral membrane tension (4). MscS-like (MSL) proteins in plants exhibit homology to the pore-lining domain of *E. coli* MscS;

outside of this region, they show diverse domains and topologies (3) (fig. S1, A and B). *Arabidopsis thaliana* mutants lacking functional MSL genes respond normally to externally applied osmotic or mechanical stresses (5).

We therefore hypothesized that MscS homologs in plants may sense and respond to rapid changes in water status (and therefore membrane tension) that are intrinsic to the plant life cycle rather than environmentally imposed. Several such events occur during the development of pollen, the multicellular haploid life stage of plants that harbors the male gametes (6). In most angiosperms, including *A. thaliana*, the last stage of pollen maturation is partial dehydration (<30% water content) (7). Once the desiccated pollen grain contacts the stigma cells of a compatible female flower, stigma exudate enters the grain and reactivates its metabolism (8). The pollen tube

germinates, breaking through the grain cell wall and proceeding via polarized tip growth toward female gametes inside the ovaries (9). The mechanical stress exerted on pollen membranes and cell walls (10, 11) and the spatially and temporally dynamic ion fluxes known to be essential for pollen grain germination and tube growth (12) suggest a role for stretch-activated ion channels (13). Mechanosensitive cation channel activities have been detected in pollen grain and tube membranes (14), but their molecular identity and physiological functions remain unknown.

*A. thaliana* MSL8 (At2g17010) transcripts were detected in mRNA isolated from floral but not leaf or root tissue (fig. S1C). In transgenic plants expressing genomic MSL8 fused to green fluorescent protein (*gMSL8-GFP*) under the control of native sequences, fluorescence was observed inside half of the pollen grains within the anthers of the hemizygous first transformed T1 generation (Fig. 1A). *gMSL8-GFP* signal was observed in tricolored and mature pollen (Fig. 1, B to F) (6) but not in any other tissue. MSL8 transcripts were identified in an RNA-sequencing data set from mature, dry pollen (15) (fig. S1D). Phylogenetic analysis suggests that male-specific expression of MSL genes evolved in both monocot and dicot lineages (fig. S2).

MSL8-GFP expressed from endogenous sequences localized both to the plasma membrane and to endomembrane compartments in pollen grains, and upon germination was mobilized to the tube periphery (Fig. 1, G and H), as did MSL8-YFP (yellow fluorescent protein) expressed from the strong pollen-specific promoter *LAT52* (Fig. 1I) (16). MSL8-YFP colocalized with the pollen plasma membrane protein CPK34 (17) but not with an endoplasmic reticulum marker (maximum Pearson's correlation coefficients of 0.66 and 0.09, respectively) (Fig. 1, J to L, and fig. S3), and there was no substantial overlap with Golgi or vacuole markers (fig. S4). A similar internal localization pattern has been observed with other pollen plasma membrane proteins (18, 19).

Department of Biology, Washington University in Saint Louis, Saint Louis, MO 63130, USA.

\*Present address: University of Miami, Miller School of Medicine, 1600 NW 10th Avenue, Miami, FL, USA. †Corresponding author. E-mail: ehaswell@wustl.edu



## Methane metabolism in the archaeal phylum Bathyarchaeota revealed by genome-centric metagenomics

Paul N. Evans *et al.*  
*Science* **350**, 434 (2015);  
DOI: 10.1126/science.aac7745

*This copy is for your personal, non-commercial use only.*

If you wish to distribute this article to others, you can order high-quality copies for your colleagues, clients, or customers by [clicking here](#).

Permission to republish or repurpose articles or portions of articles can be obtained by following the guidelines [here](#).

**The following resources related to this article are available online at [www.sciencemag.org](http://www.sciencemag.org) (this information is current as of February 23, 2016):**

**Updated information and services**, including high-resolution figures, can be found in the online version of this article at:  
</content/350/6259/434.full.html>

**Supporting Online Material** can be found at:  
</content/suppl/2015/10/21/350.6259.434.DC1.html>

A list of selected additional articles on the Science Web sites **related to this article** can be found at:  
</content/350/6259/434.full.html#related>

This article **cites 85 articles**, 43 of which can be accessed free:  
</content/350/6259/434.full.html#ref-list-1>

This article has been **cited by 1** articles hosted by HighWire Press; see:  
</content/350/6259/434.full.html#related-urls>

This article appears in the following **subject collections**:  
Microbiology  
</cgi/collection/microbio>